Design and Performance of a Non-Contacting Probe for Measurements on High-Frequency Planar Circuits

Samuel S. Osofsky, *Member, IEEE,* and S. E. Schwarz, *Fellow, IEEE*

Abstract—**Optimal design of a non-contacting magnetic probe for measurements on the interior of planar high-frequency circuits has been studied, and performance of the probe has been determined. The probe is a relatively simple device that may find uses in circuit design and optimization, troubleshooting, and production testing. In the present work we have studied its design by means of enlarged models tested at frequencies 100 times lower than those of the actual intended use. The nature of its errors has been investigated, and some techniques for error reduction have been found. The accuracy of measurements on circuits with SWR < 3.0 is typically 0.8 dB in magnitude and 7° in phase. *S*-parameter measurements on general 2-ports can also be made by using the probe at several different positions on the associated transmission lines. This technique effectively eliminates the problem of de-embedding that arises in other kinds of *S*-parameter measurements. Examples of measurements with the large model probe are presented and compared with theory. Performance appears to be acceptable for the intended applications. The probe has been designed with eventual microfabrication in mind, but difficulties in this final step remain to be resolved.**

I. Introduction

IN 1990 the 36th Annual Conference of the Automatic Radio Frequency Techniques Group had, as its theme, "On-Wafer Measurements." In the past, the standard tool for connection to MMIC's has been the contacting coplanar probe [1]. Most papers at the ARFTG conference dealt with the use of such probes, involving improvements of their frequency range and calibration methods [2]–[5]. However, probes of this kind are unsuitable for measurements at interior points of a circuit, not only because the necessary contact pads are usually absent, but also because connecting the probe to an interior point of a circuit would greatly disturb the way the circuit operates.

Manuscript received June 27, 1991; revised January 21, 1992. This work was supported by the National Science Foundation and the U.S. Army Research Office.

S. S. Osofsky was with the Department of Electrical Engineering and Computer University of California at Berkeley, Berkeley, CA 94720. He is presently with The Aerospace Corporation, M/S 1/11, 2350 East El Segundo Blvd., El Segundo, CA 90245.

S. E. Schwarz is with the Department of Electrical Engineering and Computer Science, University of California at Berkeley, Berkeley, CA 94720.

IEEE Log Number 9200858.

As an alternative, measurements at internal points of an operating circuit can be made by the electro-optic probing method [6]–[11]. This method provides a very wide bandwidth and good signal sensitivity. However, in many cases a fairly complicated laser system has been used. It would be simpler to use an electromagnetic probe, analogous to those used in waveguides. One earlier effort in this direction used the center conductor of a coaxial cable to capacitively couple to a microstrip under test [12]. However, such probes appear to be incompatible with the small dimensions of MMIC's. In earlier work we have described a non-contacting magnetic field probe that is thought to be practicable for use with present-day monolithic circuits [13], [14]. This work has now been refined and extended, in order to optimize the probe design and determine its capabilities. Our principal design technique has been the use of large-scale models, which can be conveniently constructed and tested in the 0.1–0.3 GHz range. The ultimate goal, however, is construction of probes useful at 20 GHz or higher. For this reason we have confined our efforts to designs that conceivably could be constructed on a scale one hundred times smaller than our models', by means of microfabrication technology. The experimental results to be described in this paper are obtained at the lower scale model frequency. However, it is believed that similar results can be obtained at higher frequencies if one can microfabricate identical probes on a smaller scale.

II. General Characteristics of the Probe

We desire a probe capable of accurate measurements of amplitude and phase at interior points of a circuit. Ideally, it should be capable of measurements on both microstrip and coplanar waveguide (CPW), and should have the largest bandwidth possible. Furthermore, it should disturb the operation of the circuit under test to a minimal degree, and it should respond as little as possible to radiation originating at points in the circuit other than that under test. Both of the latter requirements imply that the probe be as small as possible compared with wavelength. We envision the maximum dimension of the eventual 20-GHz probe to be on the order of 150 microns. (Such a size permits measurements on a portion of a transmission line about 150 microns in length.) Thus the design of the

probe must be amenable to realization through microfabrication techniques.

The probe described here is an improved version of the non-contacting magnetic field probe described earlier [14]. It consists of two loops and has the physical form of a magnetic quadrupole, as shown in Fig. 1. Its field configuration matches the fields of both microstrip and CPW, as shown in Fig. 2. In either case, the waveguides' magnetic field goes up through one loop and down through the other. Because of the loops' configuration, their contributions add. Signals induced in the two loops by a nearly uniform field coming from a distant source, such as another waveguide in the microcircuit, tend to cancel.

The probe design arrived at, using both theory and scale-model experiments, has (in the scale of the model) a loop length of 15 mm while the width of each loop is 7 mm, resulting in a probe that is nearly square in shape. The width of the metal strips that outline the loop is approximately 0.25 mm. The center conductor width of the circuit under test is assumed to be 5 mm or less, corresponding to 50 microns for circuits in the 15–20 GHz range. A probe with a larger loops would have greater magnetic field sensitivity, but inferior far-field radiation rejection. The feed waveguide connecting the probe to the measuring instrument is a coplanar waveguide. Tests at scale-model frequencies showed the need for a box metal waveguide to partially shield the feed CPW. To avoid antenna-like pickup, it is important that the outer planes of the feed CPW be well-connected to the box metal waveguide.

A typical measurement configuration is shown in Fig. 3. The current induced in the probe passes through the CPW transmission line to a spectrum analyzer. By this means, measurements of current amplitude can be made. To make phase measurements, a reference signal of the same frequency and adjustable phase is added to the probe signal. The reference signal's phase is varied until the amplitude seen by the spectrum analyzer is maximum. The phase at the point of measurement is then compared with that at some other point of the circuit chosen as the reference. Thus the inherent phase delays of the probe and its transmission line are of no concern.

Ideally the probe couples only to the magnetic field, and thus the current, on a transmission line. On a transmission line with reflection coefficient ρ and with an incoming wave of unit amplitude, the signal of magnetic origin S received by the spectrum analyzer has the form

$$S(z) = AI(z) \tag{1}$$

where A is the magnetic field coupling coefficient and z is the position of the probe along the line, relative to some arbitrary point. A typical scale-model experimental measurement of the phase of S and its absolute square $|S|^2$ on a loaded microstrip is shown in Fig. 4. The probe is a 100× scale model used at 0.280 GHz, simulating an actual probe to be used at 28 GHz. The power extracted from the waveguides of these dimensions is typically

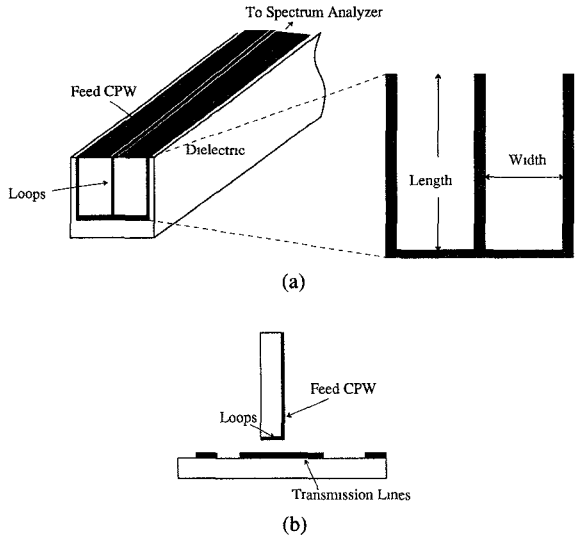

Fig. 1. (a) Double-loop magnetic-field probe. (b) Probe in position over circuit under test.

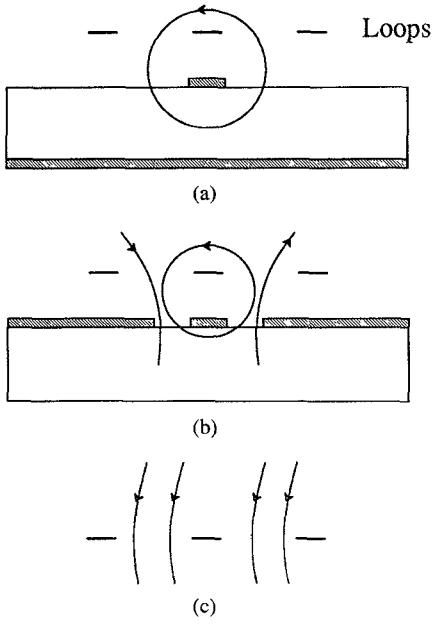

Fig. 2. Double-loop magnetic probe coupling to magnetic fields of (a) microstrip, and (b) coplanar waveguide. Radiation arriving from a distant source, as in (c), interacts with the two loops in such a way that their contributions tend to cancel.

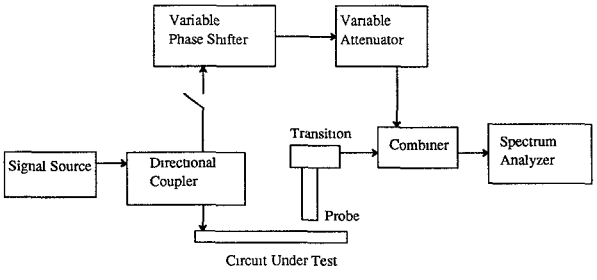

Fig. 3. Configuration for measurements of magnitude and phase.

about 25–40 dB below the power of the signal on the waveguide under test, producing a minimal effect on the circuit being tested. If we assume that $I(z) = M_o(e^{-k_g z} -$

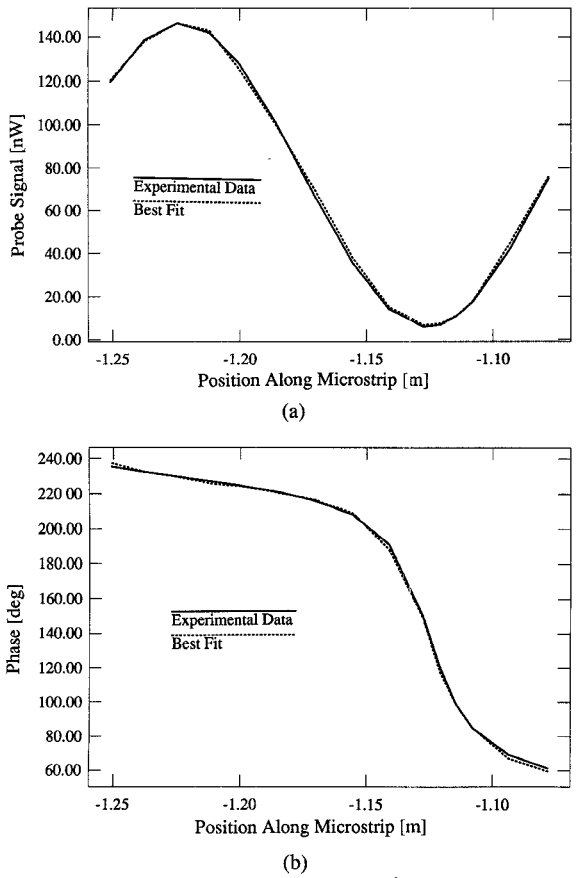

Fig. 4. Experimental and best-fit curves of (a) The square-magnitude and (b) The phase of a standing wave. The measurement was made at 280 MHz using a scale model probe placed at a height of 2.4 mm above a microstrip having a center conductor width of 5 mm, and a dielectric with $\epsilon_r = 12$ and thickness 6.35 mm.

$\rho e^{k_g z}$) with k_g assumed real, the current magnitude M and phase Φ on the transmission line are given by

$$M(z) = M_o[1 + |\rho|^2 - 2|\rho| \cos (2k_g z + \phi_\rho)] \quad (2)$$

and

$$\Phi(z) = \Phi_o + \tan^{-1} [-(\text{SWR}) \tan (k_g z + \phi_\rho/2)]. \quad (3)$$

Here SWR is the standing wave ratio, given by

$$\text{SWR} = \frac{1 + |\rho|}{1 - |\rho|} \quad (4)$$

which, like k_g, M_o, ρ ($= |\rho| e^{j\phi_\rho}$), and Φ_o, are the quantities we wish to determine by means of the measurement. Accordingly we construct a least-squares fit of (2) and (3) to the experimental data, by adjusting the values of SWR, k_g, Φ_o, and ϕ_ρ. The experimental and best-fit curves can be made to coincide quite well. However, this does not mean that the best-fit values of M_o, ρ, etc. are correct. The subject of errors will be discussed below.

In an actual measurement on an MMIC, other waveguides may be present, parallel to the one on which current is being measured. In order to avoid contamination of the measurement, the probe should have as little sensitivity as possible to such neighboring sources. Fig. 5 shows the signal received by the scale-model probe as it

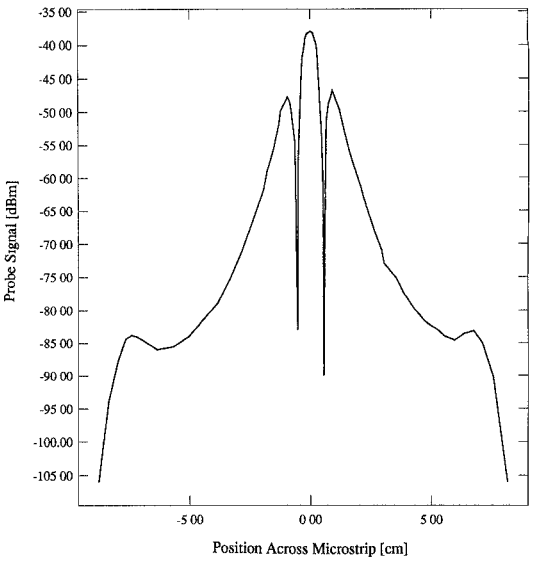

Fig. 5. Transverse pattern of an open-circuited microstrip, taken at a current maximum. The measurement was made at 150 MHz at a height of 2.4 mm above a microstrip with center conductor width 5 mm, and a dielectric with $\epsilon_r = 12$ and thickness 6.35 mm. At ± 6 cm, the probe starts to move off of the finite microstrip ground plane. The peaks at each edge of the pattern reveal that currents flow on the edges of the ground plane.

is moved from side to side across a microstrip at the position of a current maximum. We refer to this as a transverse pattern, because the probe is moved transversely to the direction of propagation on the waveguide under test. At a distance of 3 cm (on the scale of the model) from the waveguide, the signal is down by 34 dB. This indicates the rejection of a parallel waveguide located 300 microns from the one under test, when scaled to 15 GHz measurements on a microcircuit. (Of course lines closer together than 300 microns can be measured, with reduced rejection. Pickup from adjacent lines can be further reduced by reducing the dimensions of the probe, if reduced sensitivity can be tolerated.) Interestingly, small peaks are observed at ± 6 cm from the center conductor of the microstrip, corresponding to the edge of the finite microstrip ground plane. The presence of these peaks reveals that a certain amount of current is present at the edges of the ground plane. This is an observation that would be difficult to make by other techniques.

The tri-lobed form of Fig. 5 can be understood using Fig. 2. The probe signal is maximum over the center of the waveguide, where the field strength is equal in both loops but opposite in direction. As the probe moves across the waveguide, the direction of the field through the loops changes to the same direction through both loops; cancellation occurs, and an output null is observed. As the probe moves further away from the center conductor, the magnetic field goes mainly through one loop. A secondary maximum is then observed. Then as the probe moves even further away from the waveguide, the field through the loops lessens and the output signal continues to decrease.

Measurements on lines with high SWRs reveal that the form of the transverse pattern varies with longitudinal po-

sition on the line. The transverse pattern obtained at a current minimum, shown in Fig. 6, is quite different from that obtained at the current maximum (Fig. 5). This observation reveals that there is an unwanted contribution to the observed signal arising from electrostatic pickup. This contribution is normally less than the magnetic signal for which the probe is designed, but at a point on a transmission line corresponding to a current minimum, the magnetic signal is reduced and the effect of the electrostatic signal, which is maximum at that point, becomes apparent. To describe this effect, (1) is changed to

$$S = AI(z) + BV(z). \tag{5}$$

Here, B is an electric-field coupling coefficient, where $|B|Z_0 << |A|$. Both coupling coefficients can be calculated using quasi-static theory. Equivalent circuits, such as Fig. 7, can be constructed for the probe's geometry. The probe is divided into 10 strips with each strip having a resistance, an inductance, and a capacitive coupling between the center of the strip and the transmission line. The inductances are found using standard methods for planar inductors and the capacitances from finite-difference methods [15], [16]. V_e is the voltage on the transmission line, giving rise to the electrostatic signal through the several capacitances. The voltage induced in loop i by magnetic coupling, V_{mi}, is found by calculating the appropriate mutual inductance and applying Faraday's Law. (The voltages induced in the two loops are identical when the probe is centered on the line, but not when it is moved from side to side.)

From the circuit of Fig. 7 we verify that to a good approximation B is real and A is imaginary; this will be assumed throughout. Using the model of Fig. 7, together with the electrostatic and magnetostatic calculations needed to find the variation of the sources representing electric and magnetic pickup, we can then predict the variation of the measured signal as the probe is moved from side to side. Fig. 8 shows a comparison of the calculated and measured transverse patterns at the current minimum, and Fig. 9 compares the calculated and measured transverse patterns at the current maximum. The magnitudes of the "calculated" curves in both Fig. 8 and Fig. 9 were obtained by equating the calculated and measured amplitudes of the peak of Fig. 9. The shapes of the two patterns, especially the positions of the deep nulls, match very well. This verifies our interpretation of the observed phenomena as arising from the interplay of magnetic and electric pickup, and shows that electrostatic and magnetostatic calculations correctly predict the relative contributions of the two components of the signal.

The presence of electrostatic coupling gives rise to significant potential errors, as illustrated in Fig. 10(a). The curve marked "expected" is the curve which we believe would be obtained using an ideal magnetic probe, that is, a probe that has a value of A the same as the actual probe being used, but no electric sensitivity, so that $B = 0$. (The calculation of the "expected" curve is not very simple,

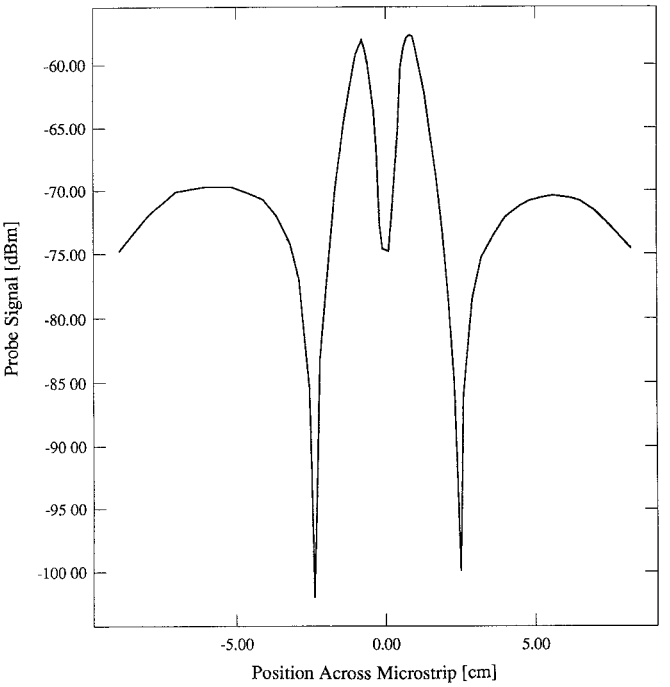

Fig. 6. Dual-lobed transverse pattern obtained with the same microstrip as Fig. 5, observed at a current minimum. The two lobes arise from capacitive coupling between the metal strips which outline the loops and the microstrip.

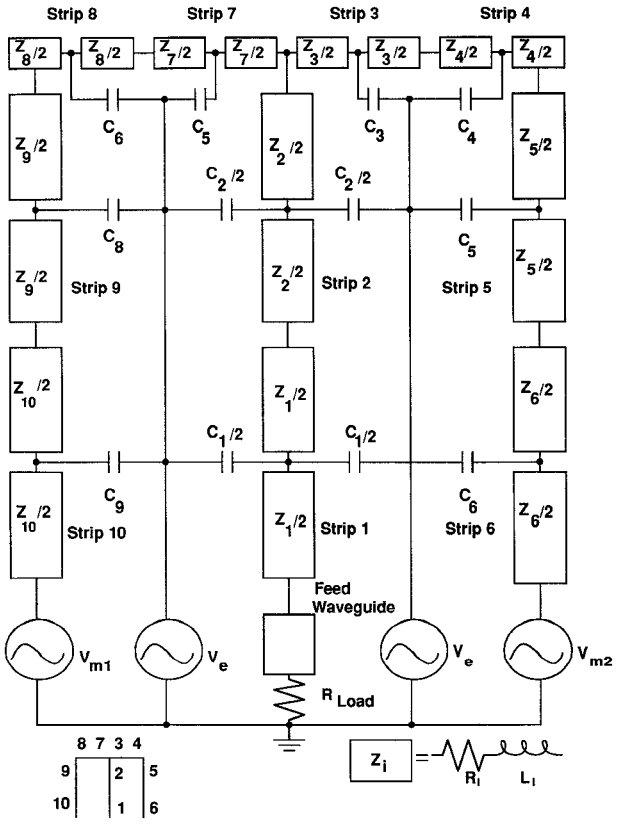

Fig. 7. Equivalent circuit modeling the magnetic and electric contributions to the probe signal. The values of the circuit elements can be calculated from electrostatic and magnetostatic theory.

but it seems unnecessary to go into its details here. Suffice it to say that using our knowledge of the actual SWR on the line—1.36, known because the termination is known—

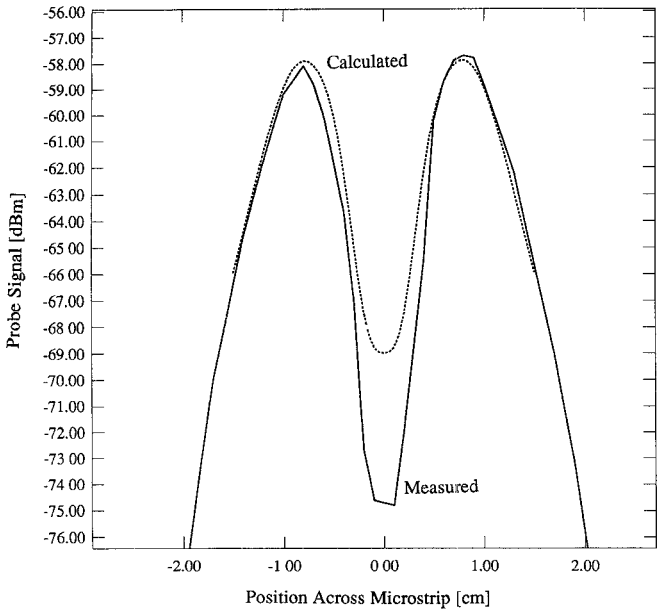

Fig. 8. Comparison of the calculated and measured transverse patterns for the case of Fig. 6.

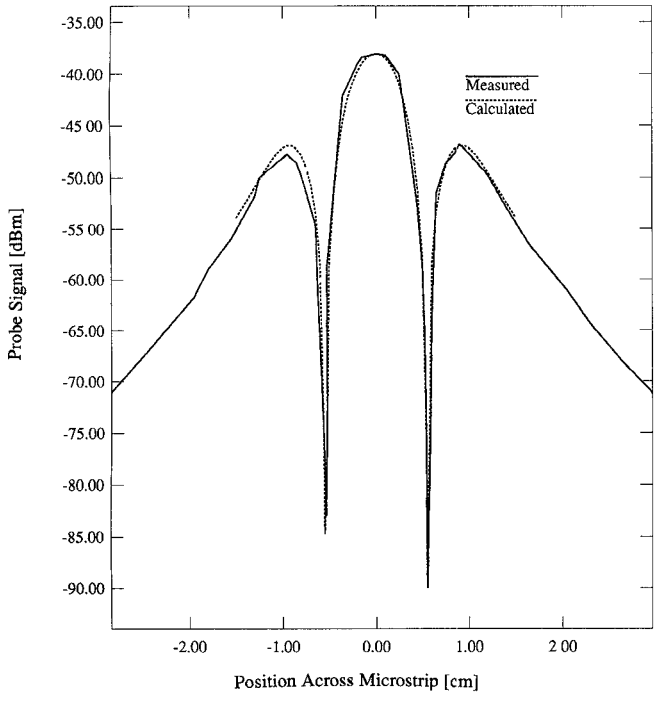

Fig. 9. Comparison of the calculated and measured transverse patterns at a current maximum for the same case as Fig. 5.

and several calibration measurements, the "expected" curve can be extracted.) The curve marked "measured" is the best fit to actual experimental data, in which electric coupling is present. At some positions the electric signal contributes constructively and at other points destructively, but the overall effect is that although the curve remains sinusoidal, it is shifted in position and increased slightly in magnitude. Thus the raw data suggest that the standing-wave pattern is different from what it actually is.

It is not possible to eliminate this error by including the

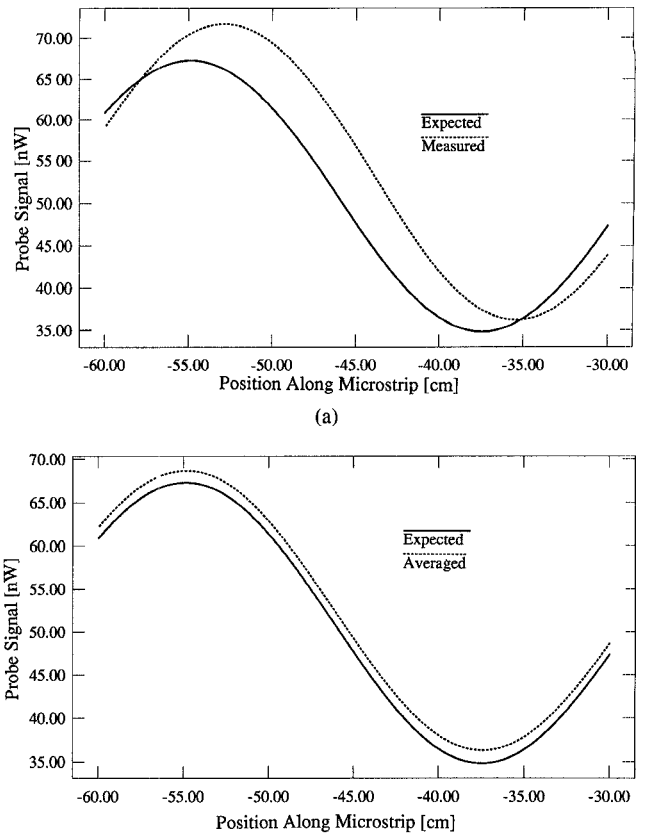

Fig. 10. Comparison of (a) the expected and measured standing wave along a microstrip having a SWR = 1.36 and (b) comparison of the expected standing wave with that obtained with the probe-reversal technique. The averaged wave in (b) was found by taking the data of Fig. 10(a), turning the probe around, re-measuring the standing wave, and then averaging the values of the two standing waves. The error caused by the parasitic electric field coupling is greatly reduced.

electrostatic contribution, because one does not know, *a priori*, the impedance at the point of measurement; without this knowledge, the size of the electric contribution cannot be found, even though the properties of the probe are completely known. However, error from this source can be largely removed through the expedient of making two measurements at the point of interest, between which the position of the probe is rotated around a vertical axis through 180°. Reversing the position of the probe reverses the algebraic sign of A with respect to B, so that taking the average of the two measurements reduces the error. If the voltage at the point of measurement is V and the current is I, the "correct" measurement is $|S|^2 = |A|^2|I|^2$. With the interfering electric pickup present, a single measurement gives the somewhat erroneous result

$$|S|^2 = |A|^2|I|^2 + |B|^2|V|^2 + 2\,\mathrm{Re}\,(ABVI) \quad (6)$$

Averaging two measurements with probe reversal, however, results in

$$|S|^2 = |A|^2|I|^2 + |B|^2|V|^2 \quad (7)$$

which is close to the ideal result, since $|B|Z_0 \ll |A|$. The effectiveness of this technique is seen in Fig. 10(b). In this figure, the curve marked "averaged" is the average

of the two best-fit curves, the first of which is a fit to experimental data, and the second of which is a fit to experimental data with the probe rotated 180°. Error in the position of the waveform is eliminated, although a small increase in the apparent magnitude of the signal still remains, arising from the term containing $|B|^2$ in (7).

III. Measurements of S-Parameters

Until now we have dealt with individual measurements of currents at a given point, such as might occur in probing an MMIC. However, the probe can also be used to make S-parameter measurements of circuit components, or of subcircuits within an MMIC. In order to determine a reflection coefficient, it is necessary to measure complex current at two different positions. Measuring the two S-parameters of a symmetric, reciprocal 2-port requires complex measurements at four positions—two on each side of the 2-port circuit. In the case of a general 2-port, determination of the four S-parameters requires complex measurements at four positions, with the output of the unknown 2-port terminated in some load, followed by four more measurements, with the output terminated by a different load. Conveniently, the actual values of the loads need not be known, which greatly simplifies the problem of de-embedding. In principle, it is only necessary that the loads be different. However, their values do affect the accuracy of the resulting measurements, as explained in the following section.

As an example of a symmetric, reciprocal 2-port, let us consider a low-impedance section in a microstrip. This section has larger width than the 50 Ω main waveguide, as shown in Fig. 11(a). Four measurements of magnitude and phase are made, at two positions on one side of the 2-port and at two positions on the other side, at each frequency. The measurements determine the unknown traveling waves at the reference planes of the 2-port and thus S_{11} and S_{21} can be found. Theoretical values of the S-parameters have been calculated by means of Touchstone (using the full model for abrupt changes in width) and are shown for comparison [17]. The measured values of $\angle S_{21}$ are within a few degrees. The measured values of $\angle S_{11}$ are somewhat more in error and tend to be more negative than the expected value of $\angle S_{11}$. The errors in S_{11} probably occur because $|S_{11}| < |S_{21}|$ for the example chosen. (Note that if $|S_{11}|$ were actually zero, its measured phase angle would be entirely determined by the errors.) The reason that the measured values of $\angle S_{11}$ tend to be consistently displaced in the negative direction will be discussed in the following section.

IV. Errors

The accuracy of the measurements is limited by several types of error: (a) uncontrolled variations in the physical position of the probe; (b) disturbance by the probe of the circuit being measured; and (c) non-ideal behavior of the probe itself, especially its undesired electrostatic pickup. As regards the first, it is particularly important that the probe be maintained at a constant height above the circuit under test. In our large scale-model apparatus, the probe's measured values are repeatable within ±0.075 dB and ±0.75°. Better accuracy may be possible at higher frequencies where the weights of the components are insignificant and electro-mechanical positioners can be used.

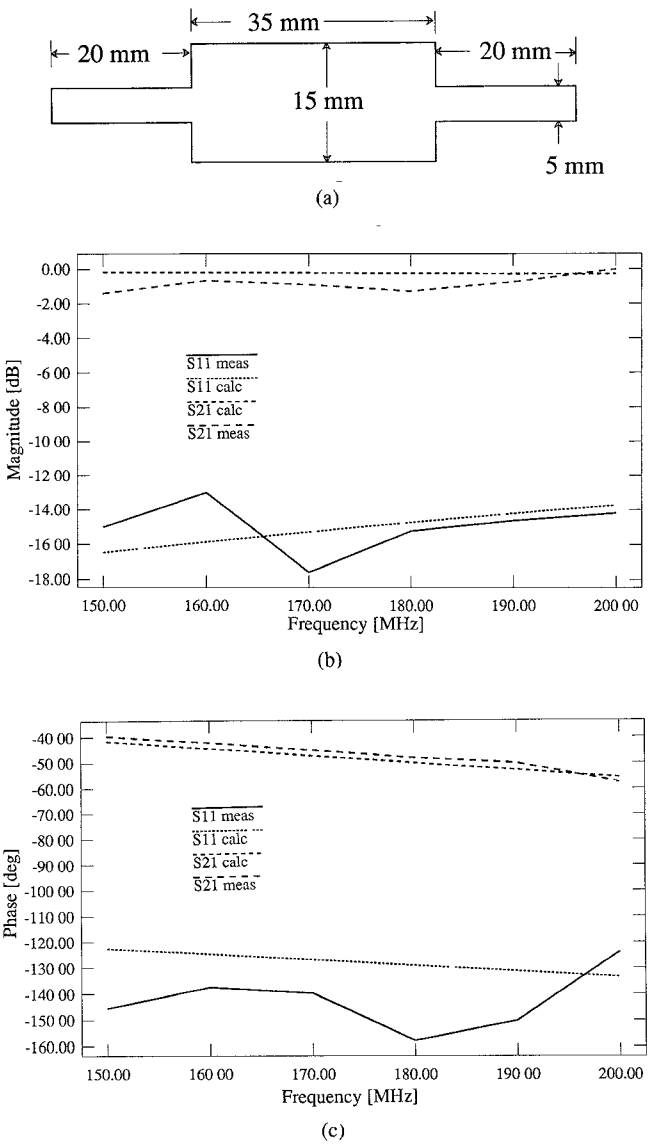

Fig. 11. Comparison of measured and calculated S-parameter (b) magnitudes and (c) phases for the low-impedance section shown in (a). The reference planes are chosen to be 20 mm from each edge of the discontinuity. The dielectric has $\epsilon_r = 12$ and thickness 6.35 mm.

It is inevitable that the probe will disturb the circuit under test to some extent. To estimate this effect, the probe was placed at various positions along a microstrip while the reflection coefficient at its input was observed with a network analyzer. Typically the probe changes $|S_{11}|$ by less than 0.04. In especially critical cases this influence on the circuit can of course be reduced by increasing the distance of the probe from the microstrip, although with loss of sensitivity.

As to the errors inherent in the probe itself, the possibility of radiative pickup has already been mentioned. Al-

though the probe's size is small compared to wavelength, it is still capable of acting like a small receiving antenna. One effect of this pickup is that in general, the probe's sensitivity is not limited by thermal noise, but rather by random radiation picked up from other elements in the circuit, which creates a floor level below which meaningful measurements cannot be made. The side lobes seen at ± 5 cm from the center conductor in Fig. 6 indicate the level of this background. These lobes are approximately 30 dB below the maximum peak of Fig. 5. Thus measurements can only be made where signal levels are somewhat above the pickup "floor." A conservative estimate is that satisfactory measurements are possible when the current at the point being measured is within about 20 dB of the maximum current that occurs in the circuit.

The most important source of error is probably electrostatic pickup. One may attempt to reduce this pickup through modification of the probe design, but tradeoffs are required with other types of error. Increasing the width of the loops increases the ratio of magnetic to electric coupling, but also increases pickup of radiated signals. Reducing the width of the metal conductors reduces capacitive pickup, but increases the conductors' resistance and self-inductance. Experience indicates that the dimensions of the square probe described in Section II are a suitable compromise at the 0.1–0.3 GHz scale. With a given probe design, the error from electrostatic pickup can be reduced by rotating the probe and averaging. The improvement obtained from this extra step was shown in Fig. 10.

In general, errors are more significant when SWR is large, because of the possibility that current may be small at the position chosen for measurement. When the SWR is less than 3.0 and frequency (for the scale model) is less than 0.30 GHz, and the rotation averaging method is used, we find that the maximum amplitude error is less than 0.8 dB, and phase errors are less than $\pm 7°$. If the position of measurement is not near a current minimum, the error will be less. Measurements at lower frequencies and on lines with lower SWR will also experience smaller errors.

Some additional comments can be made about S-parameter measurements. Four to eight separate measurements of complex current are required, each of which may have various errors. Unfortunately the measured S-parameter values tend to be surprisingly sensitive to small errors in the individual current measurements. As an example, let us consider a purely theoretical experiment involving a length of 50 Ω transmission line between two arbitrarily chosen reference planes. The S-parameters of this section of line are of course known, as are the values of current and voltage at four points outside the section, which are chosen for measurement. These values are then randomly perturbed ± 0.1 dB and $\pm 0.5°$, and the S-parameters are recalculated from these perturbed "measurements." The magnitude error between the ideal value of S_{21} and the value of S_{21} calculated from the perturbed currents is found to be on the order of 0.5 dB, and the phase error caused by these small perturbations is as large as 6°. Evidently measured S-parameters, especially their phase angles, can be quite sensitive to small errors in the current measurements. Random errors, such as those from positioning, can be averaged out by taking repeated measurements, but systematic errors will persist.

The effect of electrostatic pickup is fortuitously less significant when S-parameter measurements are being made. As we have seen, the effect of electrostatic pickup is to shift the observed standing-wave pattern (that is, the graph of $|S(z)|^2$ vs position) with respect to z, and increase its amplitude slightly. It can be shown that the shift in position is independent of the value of SWR. Therefore the shift is the same on both sides of the 2-port being measured, and has the same effect as moving both reference planes by the same distance. Doing this has no effect on the phase angles of the off-diagonal elements of the S-matrix, so those measurements are unaffected by the electrostatic pickup. However, the phase angle of the diagonal elements will be systematically either increased or decreased depending upon which way the probe is oriented with respect to the waveguide under test. The systematic displacement in the negative direction of $\angle S_{11}$ in Fig. 11 arises from this effective shift of the reference planes. The situation as regards the magnitudes of the S-parameters is slightly different. If electrostatic pickup had the effect of increasing the magnitudes of all measurements by the same factor, its effect on measurements of $|S_{11}|$ and $|S_{21}|$ would disappear. However, the electrostatic errors in magnitude of the off-diagonal elements do change slightly in response to changes in SWR, and since SWR is different on the two sides of the 2-port, complete cancellation of the errors in magnitude does not occur. Nonetheless, partial cancellation does take place, with the result that errors in $|S_{11}|$ and $|S_{21}|$ are less than errors in individual current measurements.

In general, the accuracy of S-parameter measurements will depend on the SWRs present on the lines and the positions of measurement. If SWR is low, magnitude measurements will not vary much, especially near current maxima and current minima, and magnitude errors, being comparable with changes due to position, will be quite significant. On the other hand, if an SWR is high, phase angle may change slowly with position, especially near current maxima; under these conditions, phase errors will be especially significant. To obtain good results, the measurement points should avoid the vicinity of current maxima and minima.

V. Conclusions

The probe we have described is a simple device that is capable of useful measurements on planar circuits. Although it is not free of errors, there should be many applications for which it is well suited. For example, in production testing high accuracy may not be required, while the fact that the probe is non-contacting should make it easy to move from circuit to circuit quickly. (Furthermore, similar probes could used to inject signals *into* circuits under test, so that rf testing might be accomplished

without the need for any rf contacts.) In circuit design work, the probe could be used on prototype circuits to verify circuit operation and find defects. Provided that SWRs are less than 3.0, magnitude accuracy better than 0.8 dB and phase accuracy better than 7° can be expected. In addition, the probe can be used for experimental determination of *S*-parameters, for 2-ports of arbitrary complexity, without any problems of de-embedding. Magnitudes of measured *S*-parameters are typically accurate to within ± 1.0 dB and phase angles of *S*-parameters typically within 5°, provided that the magnitude of the matrix element being measured is not too small. When the magnitude of an *S*-matrix element is small compared with unity, measurements are subject to greater error.

The major problem remaining is that of microfabricating the probe on a scale 100 times smaller than the model we have tested. This is difficult because metal must be deposited on two perpendicular surfaces, and contact made over the 90° corner between them. We have made experimental 33-GHz probes using more-or-less conventional photolithography; yield of usable probes was extremely low [14]. It appears that more innovative techniques will be required to fabricate the probes of Fig. 1 with reasonable yield [18], [19].

References

[1] K. E. Jones, E. W. Strid, and K. R. Gleason, "mm-wave wafer probes span 0 to 50 GHz," *Microwave J.*, pp. 177–183, Apr. 1987.

[2] R. Marks, "A multi-line calibration for MMIC measurements," in *36th ARFTG Conf. Dig.*, pp. 47–56, Nov. 1990.

[3] A. Davidson, E. Strid, and K. Jones, "LRM and LRRM calibrations with automatic determination of load inductance," in *36th ARFTG Conf. Dig.*, pp. 57–63, Nov. 1990.

[4] D. Williams, R. Marks, K. Phillips, T. Miers, and A. Cangellaris, "Progress toward MMIC on-wafer standards," in *36th ARFTG Conf. Dig.*, pp. 73–83, Nov. 1990.

[5] E. Godshalk, "A V-band wafer probe," presented at *ARFTG "On-Wafer Measurements II,"* Moneterey, CA, Nov. 1990.

[6] M. J. W. Rodwell, M. Riazat, K. J. Weingarten, B. A. Auld, and D. M. Bloom, "Internal microwave propagation and distortion characteristics of traveling-wave amplifiers studied by electrooptic sampling," *IEEE Trans. Microwave Theory Tech.*, vol. MTT-34, no. 12, pp. 1356–1362, Dec. 1986.

[7] J. A. Valdmanis and G. A. Mourou, "Subpicosecond electrooptic sampling: Principles and applications," *IEEE J. Quant. Electron.*, vol. QE-22, pp. 69–75, Jan. 1986.

[8] K. J. Webb, E. A. Chauchard, P. Polak-Dingels *et al.*, "A time-domain network analyzer which uses optoelectronic techniques," in *1989 IEEE MTT-S Int. Microwave Symp. Dig.*, vol. I, Long Beach, CA, June 1989, pp. 217–220.

[9] J. F. Whitaker, J. A. Valdmanis, T. A. Jackson *et al.*, "External electro-optic probing of millimeter-wave integrated circuits," in *1989 IEEE MTT-S Int. Microwave Symp. Dig.*, vol. I, F-3, Long Beach, June 1989, pp. 221–224.

[10] R. Majidi-Ahy, B. A. Auld, and D. M. Bloom, "100 GHz on-wafer *S*-parameter measurements by electrooptic sampling," *1989 IEEE MTT-S Int. Microwave Symp. Dig.*, vol. I, Long Beach, CA, June 1989, pp. 299–302.

[11] H. M. Cronson, "On-wafer *S*-parameter and waveform measurements," presented at *ARFTG On-Wafer Measurements II*, Monterey, CA, Nov. 1990.

[12] J. S. Dahele and A. L. Cullen, "Electric probe measurements on microstrip," *IEEE Trans. Microwave Theory Tech.*, vol. MTT-28, no. 7, pp. 752–755, July 1980.

[13] S. E. Schwarz and C. W. Turner, "Measurement techniques for planar high-frequency circuits," *IEEE Trans. Microwave Theory Tech.*, vol. MTT-34, pp. 463–467, Apr. 1986.

[14] S. S. Osofsky and S. E. Schwarz, "A non-contacting probe for measurements on high-frequency planar circuits," in *1989 IEEE MTT-S Int. Microwave Symp. Digest*, Long Beach, CA, vol. II, no. BB-1, June 1989, pp. 823–825.

[15] H. M. Greenhouse, "Design of planar rectangular microelectronic inductor," *IEEE Trans. Parts, Hybrids, Packag.*, vol. PHP-10, no. 2, pp. 101–109, June 1974.

[16] F. W. Grover, *Inductance Calculations.* New York: Van Nostrand, 1946, pp. 17–58.

[17] Courtesy of EEsof, Inc., Westlake Village, CA.

[18] A. T. Barfknecht, D. B. Tuckerman, J. L. Kaschmitter, and B. M. McWilliams, "Multichip packaging technology with laser-patterned interconnects," *IEEE Trans. Components, Hybrids, Manuf. Technol.*, vol. CHMT-12, no. 4, pp. 646–649, Dec. 1989.

[19] A. F. Bernhardt, A. T. Barfknecht, R. J. Contolini *et al.*, "Multichip packaging for very-high-speed digital systems," *Applied Surface Science*, vol. 46. North Holland: Elsevier Science Publishers B.V., 1990, pp. 121–130.

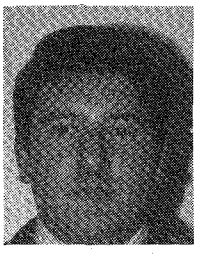

Samuel S. Osofsky (S'84–M'91) was born in Buffalo, NY on October 11, 1963. He received the B.S. degree in engineering from Harvey Mudd College in 1985, and the M.S. and Ph.D. degrees in electrical engineering from the University of California, Berkeley, in 1987 and 1991 respectively.

Dr. Osofsky is a member of the technical staff at The Aerospace Corporation. His research interests include measurements on MMIC's, microfabrication of 3-dimensional structures, modeling of microwave circuits, and live steam locomotives.

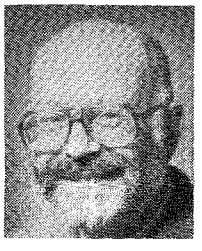

S. E. Schwarz (SM'71–F'92) was born in Los Angeles in 1939. He received the B.S. degree in physics from California Institute of Technology in 1959, the A.M. in physics from Harvard University in 1962, and the Ph.D. in electrical engineering from CalTech in 1964.

He has held positions with Hughes Research Laboratories, AT&T Bell Laboratories, and IBM Research Laboratories. Since 1964 he has been a member of the Department of Electrical Engineering and Computer Sciences at the University of California, Berkeley, where he is a Professor. His research interests currently emphasize devices and techniques for planar microwave circuits.

Dr. Schwarz held a Guggenheim fellowship in 1971–72. In 1990–1993 he occupies the President's Chair in Undergraduate Education at Berkeley.